

trajectory of an alpha particle of a given energy scattered through a particular angle. For the energy  $E_{\alpha}^0$  (hereinafter called the critical energy) at which the deviation from Coulomb scattering is first observed, the apsidal distance is found to be  $(12.5 \pm 0.2) \times 10^{-13}$  cm for the  $60^\circ$  case. This distance is significantly larger than a reasonable estimate  $(9-10 \times 10^{-13}$  cm) of the sum of the radii of the Au nucleus and the alpha particle.<sup>1</sup> A similar value,  $(12.9 \pm 0.3) \times 10^{-13}$  cm, is found for the apsidal distance at the critical energy in the  $95^\circ$  case.

Departures from Coulomb's law were observed by Bieler,<sup>2</sup> who studied the angular distribution of alphas scattered by Mg and

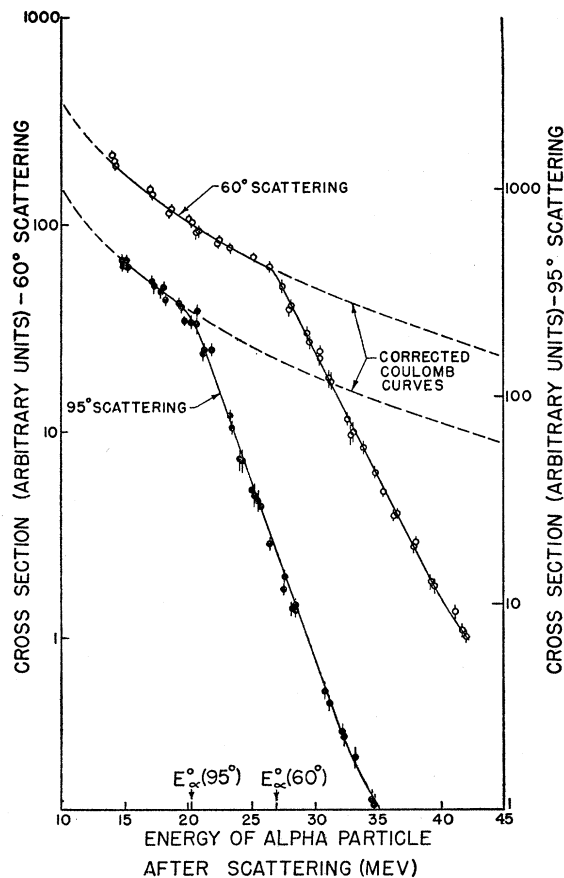


FIG. 1. Elastic scattering of alpha particles by gold. Cross section (relative) is plotted against alpha-particle energy for  $60^\circ$  scattering and for  $95^\circ$  scattering. The low-energy part of each curve is normalized to a corrected Coulomb curve (see text). The critical energy  $E_{\alpha}^0$  corresponds to the intercept of the straight line portion of the experimental curve with the corrected Coulomb curve.

Al, and by Rutherford and Chadwick,<sup>3</sup> who measured the dependence of elastic-scattering cross section upon alpha energy for Al. Data in the non-Coulomb region were very meager because of the limited range of alpha energy available, and interest in the elastic scattering of alphas by intermediate and heavy nuclei seems to have lapsed after these experiments.

The deflected alpha-particle beam of the University of Washington 60-in. cyclotron was used in the present experiments. A remotely controlled absorber was installed which could reduce the incident alpha-particle energy from 42 Mev to zero in steps of about 1 Mev. Scattered alpha particles were observed by means of a differential-range coincidence proportional-counter telescope. At each value of the incident alpha-particle energy, the number of elastically scattered alpha particles observed was normalized to the integrated beam current.

Results are shown in Fig. 1. For each scattering angle, relative elastic-scattering cross section is plotted against alpha-particle energy after scattering. Each curve is normalized to a "corrected Coulomb curve," i.e., a curve in which the energy dependence predicted by the Rutherford formula is modified very slightly to take into account a small variation in scattering angle with energy. (This variation is due to the fringing magnetic field of the cyclotron.)

At low energies, the cross section at  $60^\circ$  is seen to follow the Coulomb dependence closely. At an energy of about 27 Mev, however, the cross section begins to drop very rapidly as the alpha-particle energy  $E_{\alpha}$  is increased. The energy dependence in the range 27-40 Mev is very well represented by the simple empirical formula:

$$\sigma(E_{\alpha}) = \sigma(E_{\alpha}^0) \exp\{-K(E_{\alpha} - E_{\alpha}^0)\},$$

where  $\sigma(E_{\alpha})$  = cross section at energy  $E_{\alpha}$  (Mev),  $E_{\alpha}^0$  = critical energy =  $27.0 \pm 0.3$  Mev, and  $K$  = constant =  $0.28 \text{ Mev}^{-1}$ .

The curve for scattering through  $90^\circ$  is similar in form, the critical energy  $E_{\alpha}^0$  being lower ( $20.25 \pm 0.4$  Mev) and  $K$  being higher ( $0.40 \text{ Mev}^{-1}$ ).

Studies are in progress using other heavy elements. Preliminary results are very similar to those for Au. The critical energy  $E_{\alpha}^0$  increases with  $Z$  but the parameter  $K$  appears to be independent of  $Z$  (for a particular scattering angle) within the experimental uncertainties.

Since  $E_{\alpha}^0$  and the corresponding apsidal distance can be measured quite precisely, it seems likely that these experiments offer a sensitive means of detecting small differences in nuclear size, and we expect to explore this aspect. It is evident that strong absorption occurs when nuclear forces come into play at apsidal distances comparable to the nuclear radius. A theoretical analysis of the present results and others to be obtained should give more exact information on the nature of the interaction between alpha particles and heavy nuclei and on effective nuclear and alpha particle radii.

It is a pleasure to acknowledge valuable discussions with Dr. J. S. Blair.

\* This work was supported in part by the U. S. Atomic Energy Commission.

† Now at Brookhaven National Laboratory, Upton, New York.

<sup>1</sup> Use of  $R_n = r_0 A^{1/3}$ , with  $r_0 = 1.4 \times 10^{-13}$  cm, gives for the radius of the Au nucleus the value  $R_n = 8.1 \times 10^{-13}$  cm. Following J. M. Blatt and V. F. Weisskopf, *Theoretical Nuclear Physics* (John Wiley and Sons, Inc., New York, 1952), a value  $R_n = 1.2 \times 10^{-13}$  cm is assumed here for the effective alpha-particle radius.

<sup>2</sup> E. S. Bieler, Proc. Roy. Soc. (London) **A105**, 434 (1924).

<sup>3</sup> E. Rutherford and J. Chadwick, Phil. Mag. **50**, 889 (1925).

## Proton Distribution in Heavy Nuclei\*

M. H. JOHNSON AND E. TELLER

Radiation Laboratory, University of California, Livermore, California

(Received November 23, 1953)

THE Coulomb repulsion tends to force protons as far apart as possible, thereby lowering the proton density at the center of a nucleus. One might conclude that such an expansion would cause a proton excess on the nuclear surface. It is easy to see that the stability against  $\beta$  decay brings about the opposite result, a neutron excess on the surface.

The top part of Fig. 1 gives a qualitative picture of the average potential acting on neutrons and protons. It is assumed that the proton potential and the neutron potential are the same except for the electrostatic energy. The dashed line indicates the highest filled energy state in the Fermi distribution for both protons and neutrons. Beta stability requires that the highest filled proton state have the same energy as the highest filled neutron state (actually the proton should have 0.79 Mev more energy, a difference that may be neglected compared to the Coulomb potential in heavy nuclei). If the nuclear potential at the surface has a finite slope, the dashed line intercepts the potential at a somewhat smaller radius for protons. Consequently, the proton

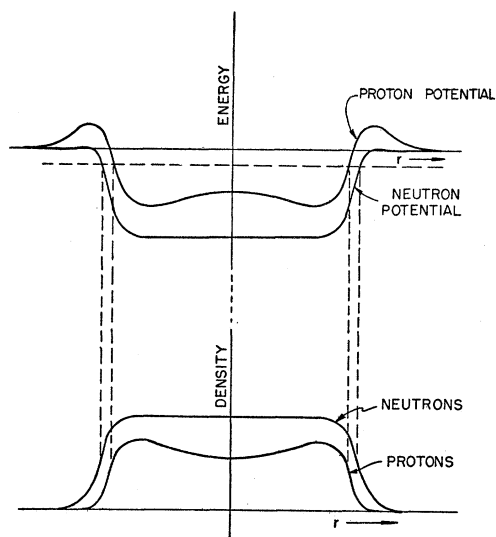


FIG. 1. Potentials and densities for protons and neutrons inside the nucleus.

distribution lies inside the neutron distribution. For the heaviest elements the difference in radii could easily be  $\frac{1}{3}$  to  $\frac{1}{2}$  the thickness of the sloping part of the nuclear potential; the latter is likely to be of the order of the meson Compton wavelength. Thus the radius of the proton distribution may turn out smaller than the neutron radius by about  $10^{-13}$  cm.

A more detailed examination of the nucleon orbits gives qualitatively the same result. The intercept of the energy level with the radial potential determines a point of inflection for the wave function; beyond this point the wave function is always convex to the axis. This point will be different for different angular momenta but will lie at systematically smaller radii for protons. In addition, the higher potential barrier for protons outside this point causes proton wave functions to vanish more rapidly than neutron wave functions. The lower part of Fig. 1 gives a qualitative picture of the proton and neutron densities within the nucleus.

In experiments with nucleons and  $\pi$  mesons which interact strongly with nuclear matter, one may find the surface of the nucleus at radii where practically no protons are present and the neutron density is well below its plateau value. In experiments with electrons and  $\mu$  mesons which interact only with the electrostatic field, one may find the smaller radii characteristic of the proton distribution.

\* Work supported by the U. S. Atomic Energy Commission.

### A New Titanium Nuclide: $Ti^{44}$

R. A. SHARP AND R. M. DIAMOND

Department of Chemistry, Harvard University, Cambridge, Massachusetts

(Received November 30, 1953)

A LONG-LIVED titanium activity has been produced by the irradiation of scandium oxide with 30-45-Mev protons. Spectroscopic analysis showed that the scandium oxide available<sup>1</sup> contained about 1 percent each of zirconium and calcium and about  $\frac{1}{2}$  percent each of thorium and combined rare earths; initial studies indicated that these impurities caused too much radioactive contamination to observe any long-lived titanium activity. The necessary scandium purification was accomplished by the development of a solvent extraction method using thenoyltrifluoroacetone (TTA).<sup>2</sup> Samples of approximately 70 mg of the purified oxide were wrapped in aluminum foil and bombarded

for  $\sim 1$  microampere hour in the internal beam of the Harvard 95-inch synchrocyclotron, yielding  $\sim 100$  dis/sec of the new activity.

After the 3.1-hour  $Ti^{46}$  and the 3.9-hour  $Sc^{43}$  and  $Sc^{44}$  activities had been allowed to decay, the target material and 10 mg of titanium metal as carrier were dissolved in boiling 6*N* HCl. Hydrogen peroxide was added to insure that all the titanium was in the (IV) state and was then destroyed by further boiling. The titanium fraction was isolated by repeated cupferron precipitation from chilled 6*N* HCl solution and subsequent extraction into chloroform.<sup>3</sup>

By a similar procedure the scandium daughter could be separated from its titanium parent, and this separation was effected several times during a period of months to the titanium fractions from targets from three bombardments. Immediately after separation, the activities of both parent and daughter fractions were followed in an argon-filled, chlorine-quenched, end-window Geiger counter, a windowless proportional counter using a mixture of 95 percent argon, 5 percent  $CO_2$  as counting gas, and a thallium-activated NaI scintillation counter.

With all counters the scandium daughter activity showed a 4-hour decay which turned over into a small amount of a long-lived component, probably because of incomplete separation of the titanium parent. The fact that approximately the same amount of 4-hour scandium activity could be separated repeatedly from the titanium fraction over a period of several months shows the presence of a long-lived parent nuclide, and the 4-hour half-life of the daughter indicates mass number either 43 or 44. Since  $Sc^{43}$  has a 1.46-Mev positron and a 1.16-Mev gamma, whereas  $Sc^{44}$  has 1.18- and 0.77-Mev positron groups and a 375-kev gamma,<sup>3</sup> an aluminum absorption curve taken with the Geiger counter and an integral gamma pulse-height curve taken with the scintillation counter on the scandium daughter showed unambiguously that the daughter was  $Sc^{44}$ . This assignment of the activity to  $Ti^{44}$  is to be expected from a consideration of beta-decay systematics.

When the Geiger and proportional counters were used, the activity of the freshly separated titanium fractions was observed to grow from just above background to the final equilibrium values with a 4-hour half-life, indicating no particulate radiation ( $< 5$  percent abundance) in the decay of  $Ti^{44}$ . Integral gamma pulse-height curves taken with the scintillation counter during the growth of the daughter activity showed the presence of an  $\sim 1.2$ -Mev gamma activity growing with a 4-hour half-life and another of  $160 \pm 60$  kev of constant intensity. The high-energy gamma is the 1.16-Mev gamma of the growing  $Sc^{44}$  activity, whereas the lower energy gamma must be associated with the  $Ti^{44}$  decay itself. Taking the counting efficiency of the 1.16-Mev gamma in the large well-type NaI crystal used as approximately equal to that of the experimentally determined average value for the 1.17- and 1.33-Mev gammas of  $Co^{60}$  and assuming that the counting effi-

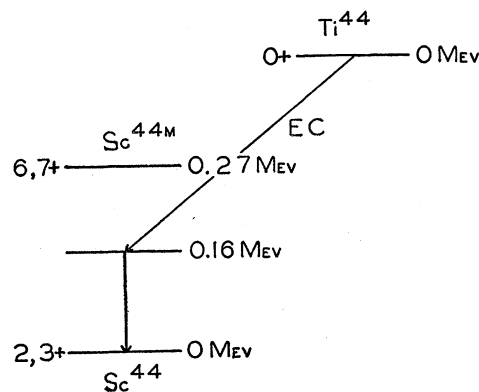


FIG. 1. Proposed decay scheme of  $Ti^{44}$ .